Paper 118

Proceedings of the Eleventh International Conference
on Computational Structures Technology,
B.H.V. Topping, (Editor),
Civil-Comp Press, Stirlingshire, Scotland

Numerical Methods for Slender Masonry Structures: A Comparative Study

M. Girardi[1], M. Lucchesi[2], C. Padovani[1]
G. Pasquinelli[1], B. Pintucchi[2] and N. Zani[2]
[1] Institute of Information Science and Technologies "Alessandro. Faedo" ISTI-CNR, Pisa, Italy
[2] Department for Constructions and Restoration University of Florence, Italy

Abstract

This paper is devoted to comparing two numerical approaches for modelling the dynamic behaviour of masonry structures. It presents the constitutive equation of masonry-like materials with bounded compressive strength and addresses the dynamic problem for both three-dimensional bodies and one-dimensional structures. The numerical methods implemented in the codes NOSA-ITACA and MADY, respectively for three- and one-dimensional structures, are outlined. With the aim of comparing the two numerical procedures, a masonry tower with rectangular cross-section is analised. The structure is subjected to its own weight and an accelerogram recorded during a real earthquake. This comparison has emphasised the importance of employing accurate constitutive models when analysing masonry structures.

Keywords: masonry-like materials, nonlinear dynamics, masonry towers, numerical methods.

1 Introduction

Numerical tools for modelling masonry buildings subjected to time-dependent loads have a proven, important role in assessing the seismic vulnerability of historical constructions. The two main aspects that need to be addressed in studying the dynamic behaviour of masonry structures are the choice of the constitutive equation for masonry materials, whose mechanical properties depend heavily on its constituent elements and the building techniques used, and the formulation of suitable numerical techniques for integrating the equations of motion.

Constitutive equations for masonry materials range from linear elastic models aiming to provide qualitative information on the behaviour of masonry structures [1], [2], [3] to elastic-plastic models directed at taking into account the strong nonlinearities

of such structures' dynamic response [4]-[9]. The constitutive equation for masonry materials proposed in [10] and [11] models masonry as a nonlinear elastic material with zero tensile strength and infinite compressive strength. This constitutive equation, which is known as the masonry-like (or no-tension) model, has been generalized in order to take into account the bounded compressive strength of masonry materials [12]. The equation has subsequently been implemented in the finite element code NOSA [12], developed at the Institute of Information Science and Technologies "A. Faedo" (ISTI-CNR) and successfully applied to the static analysis of several historical masonry buildings, and more recently to the dynamic analysis of masonry beams and towers [13], [14].

As far as numerical solution of dynamic problems is concerned, the NOSA code applies the Newmark method to integrate with respect to time the system of ordinary differential equations obtained by discretising the structure into finite elements [15], [13].

The research and development activities of ISTI-CNR are continuing within the framework of the NOSA-ITACA project [16], [17]. The project, conducted in collaboration with the Department for Constructions and Restoration (DICR) of the University of Florence and funded by the Region of Tuscany, aims to develop a new tool, the NOSA-ITACA code, stemming from integration of NOSA and the open-source graphical user interface platform SALOME [18]. An application of NOSA-ITACA to the "Rognosa" tower in San Gimignano has been presented in [16] and [19], where the tower's mechanical response to seismic actions is assessed.

Recent efforts have been directed at developing simplified constitutive models for masonry structures by representing them through one-dimensional elements. Such efforts have given rise to a nonlinear constitutive equation for beams, in which the generalized stress (normal force and bending moment) is a function of the generalized strain (extensional strain and curvature change of the beam's longitudinal axis) [20]. This constitutive model is based on the assumption that the material does not withstand tensile stresses in the longitudinal direction. Variants of the model take into account cases of unbounded as well as bounded compressive strength. The model has been extended to deal with both solid and hollow rectangular cross-sections in order to study masonry arches and freestanding towers [21], [22]. The resulting constitutive equation has been implemented in the numerical code MADY, developed at DICR to perform nonlinear dynamic analyses of slender masonry structures.

The present paper is devoted to comparing the models implemented in the two finite element codes NOSA-ITACA and MADY, which are applied to the dynamic problem of a masonry tower with hollow rectangular cross-section subjected to its own weight and an accelerogram recorded during a real earthquake. The solutions obtained via the two different models are compared in order to highlight the similarities and differences between the numerical procedures proposed.

2 Numerical modelling

In this section the constitutive equation of masonry-like materials with bounded compressive strength is recalled and the equations governing the motion of masonry structures together with the numerical techniques for their approximate solution are presented. The cases of three-dimensional bodies and one-dimensional structures are dealt with separately.

2.1 Three-dimensional bodies

The constitutive equation of masonry-like materials is based on three assumptions: infinitesimal elasticity, zero tensile strength and a normality postulate. For a more detailed treatment of this subject, refer to [10]-[12]. Herein, we recall some fundamental results on the constitutive equations of masonry-like materials with bounded compressive strength introduced in [12].

Let Sym be the vector space of symmetric tensors equipped with the inner product $\mathbf{A} \cdot \mathbf{B} = tr(\mathbf{AB})$, $\mathbf{A}, \mathbf{B} \in$Sym, with tr the trace. We denote by Sym$^+$ and Sym$^-$ the convex cones of Sym constituted by the positive and negative semidefinite tensors, respectively.

Let $\mathbb{C}$ be an isotropic fourth-order tensor called the elasticity tensor of the material, $\mathbb{C} = \frac{E}{1+\nu}\left(\mathbb{I} + \frac{\nu}{1-2\nu}\mathbf{I} \otimes \mathbf{I}\right)$, with $\mathbb{I}$ the fourth-order identity tensor, $\mathbf{I}$ the identity of Sym and $\otimes$ the tensor product defined by $\mathbf{I} \otimes \mathbf{I}[\mathbf{A}] = tr(\mathbf{A})\mathbf{I}$, for each $\mathbf{A} \in$Sym. Quantities E and ν are respectively the Young's modulus and the Poisson's ratio of the material, satisfying the inequalities $E > 0, \quad 0 \leq \nu < \frac{1}{2}$. Moreover, we denote by $\sigma_0 < 0$ the maximum compressive stress of the material and define the closed convex set of Sym, $\mathcal{K} = \{\mathbf{A} \in \text{Sym} \mid \mathbf{A} \in \text{Sym}^-, \mathbf{A} - \sigma_0\mathbf{I} \in \text{Sym}^+\}$. A masonry-like material with bounded compressive strength is completely determined by the fourth-order tensor $\mathbb{C}$ and set $\mathcal{K}$. In fact, it is possible to prove that if $\mathbf{E} \in$Sym, there exists a unique triplet ($\mathbf{T}$, $\mathbf{E}^e$, $\mathbf{E}^a$) of elements of Sym such that [23],

$$\left.\begin{array}{c} \mathbf{E} = \mathbf{E}^e + \mathbf{E}^a, \\ \mathbf{T} = \mathbb{C}[\mathbf{E}^e], \\ \mathbf{T} \in \mathcal{K}, \\ (\mathbf{T} - \mathbf{S}) \cdot \mathbf{E}^a \geq 0 \quad \text{for each } \mathbf{S} \in \mathcal{K}. \end{array}\right\} \tag{1}$$

The stress function $\widehat{\mathbf{T}}$ is defined by $\widehat{\mathbf{T}}(\mathbf{E}) = \mathbf{T}$ and tensors $\mathbf{E}$, $\mathbf{T}$, $\mathbf{E}^e$ and $\mathbf{E}^a$ are coaxial. Let $\sqrt{(\mathbf{E}^a)^2}$ denote the square root of the tensor $(\mathbf{E}^a)^2 \in$Sym$^+$ [24]. The positive semidefinite part

$$\mathbf{E}^f = \frac{1}{2}(\mathbf{E}^a + \sqrt{(\mathbf{E}^a)^2}), \tag{2}$$

and negative semidefinite part

$$\mathbf{E}^c = \frac{1}{2}(\mathbf{E}^a - \sqrt{(\mathbf{E}^a)^2}), \tag{3}$$

of $\mathbf{E}^a$ satisfy the relations [25]

$$\mathbf{T} \cdot \mathbf{E}^f = 0, \quad (\mathbf{T} - \sigma_0 \mathbf{I}) \cdot \mathbf{E}^c = 0, \tag{4}$$

and are called fracture strain and crushing strain, respectively. The material defined by constitutive equation (1) is hyperelastic [12], [23], with strain energy density

$$\psi(\mathbf{E}) = \frac{1}{2}\mathbf{E}^e \cdot \mathbb{C}[\mathbf{E}^e] + \mathbf{T} \cdot \mathbf{E}^a, \quad \mathbf{E} \in \text{Sym}. \tag{5}$$

Both $\widehat{\mathbf{T}}$ and its derivative $D_E\widehat{\mathbf{T}}(\mathbf{E})$ with respect to $\mathbf{E}$ have been explicitly calculated in [12] for three and two-dimensional cases. Here we recall how the constitutive equation (1) can be applied to the study of masonry shell structures, such as vaults, domes etc., dealt with in [12]. Consider the shell element of thickness h shown in Figure 1. Let η_1 and η_2 be an orthogonal coordinate system defined on the mean surface Σ, with $\zeta \in [-h/2, h/2]$ as the coordinate in the normal direction $\mathbf{n}$. We denote by $\mathbf{g}_1$ and $\mathbf{g}_2$ the unit tangent vectors to the η_1 and η_2 axis, respectively. The structure can be considered to be made up of the layers

$$\Sigma_\zeta = \{\mathbf{p}' = \mathbf{p} + \zeta\mathbf{n},\ \mathbf{p} \in \Sigma,\ \mathbf{n} = \mathbf{n}(\mathbf{p})\},\ \zeta \in [-h/2, h/2], \tag{6}$$

and we assume that for each $\mathbf{p}' \in \Sigma_\zeta$, $\mathbf{T}$ satisfies the condition

$$\mathbf{T}(\mathbf{p}, \zeta)\mathbf{n}(\mathbf{p}) = \mathbf{0}. \tag{7}$$

We indicate with the same symbols the restrictions of $\mathbf{E}$, $\mathbf{T}$, $\mathbf{E}^f$ and $\mathbf{E}^c$ to the two-dimensional linear space generated by $\mathbf{g}_1$ and $\mathbf{g}_2$. The explicit solution to constitutive equation (1) with $\mathbf{T}$ satisfying (7) and the derivative of $\mathbf{T}$ with respect to $\mathbf{E}$ are given in [12]. In [13] a numerical procedure is proposed with the aim of solving the dynamic problem of masonry structures via the finite-element method. This numerical procedure is now implemented in the NOSA-ITACA code, which performs the integration with respect to time of the system of ordinary differential equations obtained by discretising the structure into finite elements. At each time step, a system of the type

$$K(u_t)\ \Delta u + C\ \Delta\dot{u} + \widetilde{M}\ \Delta\ddot{u} = \Delta f, \tag{8}$$

is solved by applying the Newmark method [15]. In (8) u_t is the nodal displacement at time t, Δf is the load increment, Δu, $\Delta\dot{u}$ $\Delta\ddot{u}$ are respectively the incremental nodal displacement, velocity and acceleration, and K, C and $\widetilde{M}$ are the stiffness, damping and mass matrices of the structure. According to the Rayleigh assumption in [15], C takes the form $C = \alpha\widetilde{M} + \beta K$. Constants α and β are to be determined from the vibration frequencies of the structure considered as linear elastic and from the corresponding damping ratios. The solution to the nonlinear algebraic system obtained from (8) via the Newmark method is then calculated using the Newton-Raphson algorithm.

2.2 One-dimensional structures

Recent efforts have been directed at developing a simplified constitutive model for one-dimensional structures. This constitutive equation, applied at first to static problems [20], has been used for nonlinear dynamic analyses of slender masonry structures with simple geometries and flexural behaviour [22]. Specifically, the model, initially formulated for masonry columns, has been developed using the constitutive equation for rectangular cross-section beams, under the assumption that the material has zero tensile strength in the longitudinal direction. Variants to the model [20], [21] moreover take into account both unbounded and bounded compressive strength and in [22] the case of hollow, rectangular cross-section beams is dealt with.

The numerical method method proposed in [22] has been implemented into a finite element code, named MADY, which allows for performing nonlinear dynamic analyses of the aforementioned structures under very general load and boundary conditions, as well as in the presence of horizontal and vertical seismic excitations.

In the following, we outline the constitutive equation for hollow, rectangular cross-section beams (Figure 2) with bounded compressive strength [22] and we recall the algorithm for solving the coupled transverse and longitudinal vibrations problem.

Here we make the classical Euler-Bernoulli assumption and consider axial stresses alone. Thus, the constitutive equation of the beam can be formulated in terms of generalized stress and strain: the strain state is described by the extensional strain ε and the curvature change κ of the longitudinal axis, and the stress state is represented by axial force N and bending moment M. The material is assumed to be nonlinear elastic with zero tensile strength and maximum compressive stress σ_0.

With the aim of determining the relation between generalized stress and generalized strain, we firstly note that each longitudinal fiber $y = \overline{y}$, with $-h/2 \leq \overline{y} \leq h/2$, undergoes the axial stress

$$\sigma(\overline{y}) = \begin{cases} \sigma_0 & \text{if } \varepsilon(\overline{y}) \leq \varepsilon_0, \\ E\varepsilon(\overline{y}) & \text{if } \varepsilon_0 \leq \varepsilon(\overline{y}) \leq 0, \\ 0 & \text{if } \varepsilon(\overline{y}) > 0, \end{cases} \tag{9}$$

where, in view of the Euler-Bernoulli hypothesis, $\varepsilon(\overline{y}) = \varepsilon + \overline{y}\kappa$, ε_0 is the strain corresponding to σ_0 and E is the Young's modulus. Let us consider the neutral axis having equation $y = y_n$, where y_n satisfies the condition

$$\varepsilon + y_n\kappa = 0, \tag{10}$$

and the axis with equation $y = y_s$, where the stress reaches its limit value σ_0, with y_s satisfying the condition

$$\varepsilon + y_s\kappa = \varepsilon_0. \tag{11}$$

From (10) and (11), we get

$$y_n = -\frac{\varepsilon}{\kappa}, \quad y_s = \frac{\varepsilon_0 - \varepsilon}{\kappa}. \tag{12}$$

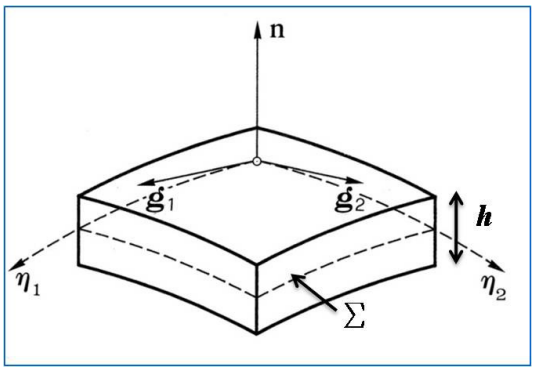

Figure 1: The shell element.

Depending on y_n and y_s, the plane (ε, κ) is divided into thirteen regions E_i, $i = 1 \ldots 13$, for each of which we have a different stress pattern, as shown in Figure 3. An explicit expression of N and M as functions of ε and κ

$$N = \bar{N}(\varepsilon, \kappa), \quad M = \bar{M}(\varepsilon, \kappa) \tag{13}$$

in each region E_i can be found in [22].

The equations of transverse and axial vibrations of a beam, which include the axial force effects are [26]

$$\overline{\rho}\frac{\partial^2 v}{\partial t^2} + \frac{\partial}{\partial z}\left(\frac{\partial M}{\partial z} + N\frac{\partial v}{\partial z}\right) - q = 0, \tag{14}$$

$$\overline{\rho}\frac{\partial^2 u}{\partial t^2} - \frac{\partial N}{\partial z} - p = 0, \tag{15}$$

where z denotes the abscissa along the beam's axis and t the time. $M(z,t)$, $N(z,t)$, $u(z,t)$ and $v(z,t)$ are the bending moment, axial force, longitudinal and transverse displacements, respectively; $p(z,t)$ and $q(z,t)$ are the axial and transverse distributed loads, and $\overline{\rho}$ the mass per unit length. The dynamic problem of the beam is governed by the equations (14) and (15) together with the strain-displacement relations

$$\varepsilon = \frac{\partial u}{\partial z}, \quad \kappa = \frac{\partial^2 v}{\partial z^2}, \tag{16}$$

and the constitutive relations (13), which are solved numerically via the MADY code. The beam is discretized into finite elements and each node has three degrees of freedom: axial and transverse displacement plus rotation. The flexural problem is addressed by using Hermite shape functions, which guarantee the continuity of both the transverse displacement and rotation, while linear shape functions are adopted for the axial displacement. Moreover, the Newmark and the Newton-Raphson methods are used to obtain the numerical solution. Lastly, the effects of viscous damping are taken into account by means of a constant damping matrix C, as in subsection 2.1. Greater details on the numerical procedure implemented in MADY are given in [22].

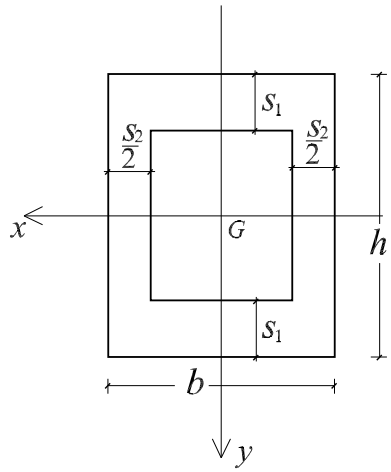

Figure 2: The beam section.

3 An application: the masonry tower

This section illustrates application of the models described in subsections 2.1 and 2.2 to the case of a slender tower with constant cross-section subjected to both its own weight and an accelerogram recorded during a real earthquake. By referring to some of the typical characteristics of ancient, free-standing towers in Italy, for the analysis we have chosen a tower with a square cross-section, 45 m in height and 6 m in width, with walls of constant 1.6 m thickness. We have assumed $E = 3000$ MPa for the Young's modulus, $\rho = 1900$ kg/m^3 for the mass density and $\sigma_0 = -1.7$ MPa for the maximum compressive stress. The first two flexural periods of the structure in the linear elastic range are $T_1 = 1.507$ s and $T_2 = 0.240$ s, and the Rayleigh damping coefficients α and β, evaluated by assuming a damping ratio $\gamma = 0.02$ over the two flexural modes T_1 and T_2, according to the formulae [26],

$$\alpha = 4\pi\gamma/(T_1 + T_2), \;\; \beta = T_1 T_2 \gamma/[\pi(T_1 + T_2)],$$

are $\alpha = 0.14383805$ s^{-1}and $\beta = 0.00132001$ s.

The structure is subjected to the horizontal component of the 1997 Nocera Umbra earthquake, whose accelerogram is reported in Figure 4, applied along the x direction; it had a duration of 41.30 s and a maximum acceleration (PGA) of 4.3192 m/s^2. The tower has been analyzed with NOSA-ITACA, using 1080 shell elements (see Figure 5, where the faces are numbered from 1 to 4 and some critical points are labelled) and with MADY, using 90 one-dimensional elements. The time step is 10^{-2} s for both NOSA-ITACA and MADY. Two analyses have been performed, considering a masonry-like material with constitutive equation (1), in the case of NOSA-ITACA, and constitutive equation of masonry beams (13), in the case of MADY.

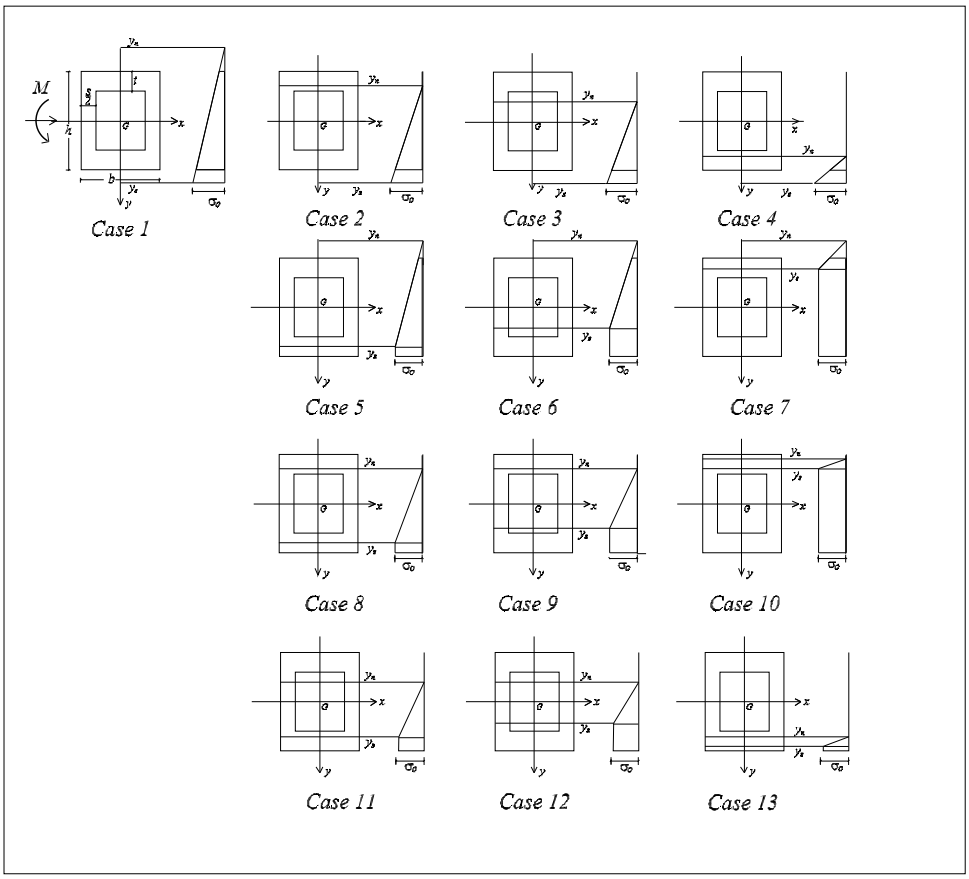

Figure 3: Patterns of stress σ in the beam cross–section.

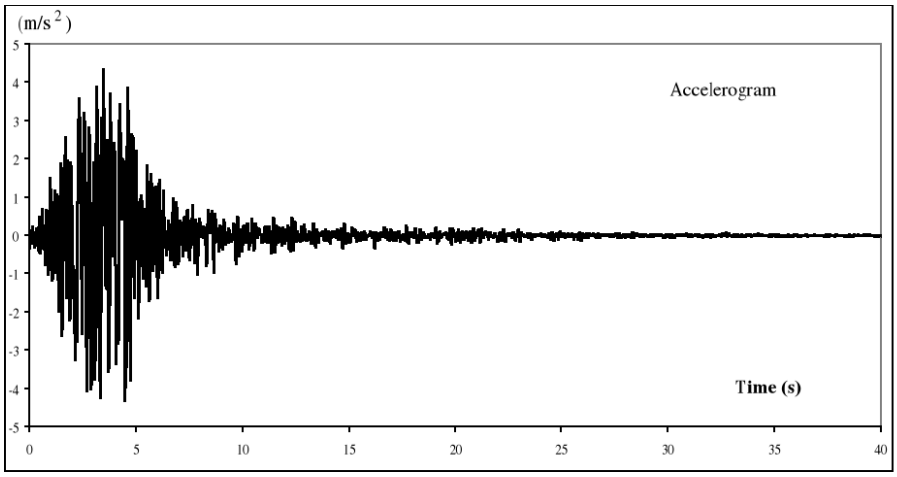

Figure 4: Accelerogram of the Nocera Umbra earthquake, 1997.

Figure 6 shows the behaviour of the relative displacement u_x of the top of the tower (point A in Figure 5) in the $x-$direction, obtained with NOSA-ITACA (black line) and MADY (red line). In Figure 7 the maximum $U(z)$ of the modulus of u_x in the cross section over the interval $t \in [0, 41.3]$, is plotted as function of the height z. Although Figure 6 shows some discrepancies between the displacements time-histories calculated via the two codes, the maximum absolute values along the tower's height are substantially coincident and clearly highlight the amplification effects of the dynamic forces in the highest part of the structure.

As for the fracture and crushing strains distributions calculated with MADY, some global parameters can be plotted to describe the damage to the structure: Figure 8 shows the ratio F_V/T_V, between the volume F_V of the cracked portion and the total volume T_V of the tower, as function of time. Figure 9 shows instead the quantity C_V/T_V vs. t, with C_V the volume of the crushed regions.

The results of the NOSA-ITACA code are summarized in Figures from 10 to 14. For $\mathbf{g}_1$ and $\mathbf{g}_2$, respectively the unit vectors of the horizontal tangential axis and z-axis (Figure 5), the components of the fracture strain $\mathbf{E}^f$ with respect to $\mathbf{g}_1$ and $\mathbf{g}_2$ are E^f_{11}=$\mathbf{g}_1 \cdot \mathbf{E}^f \mathbf{g}_1$, E^f_{22}=$\mathbf{g}_2 \cdot \mathbf{E}^f \mathbf{g}_2$ and E^f_{12}=$\mathbf{g}_1 \cdot \mathbf{E}^f \mathbf{g}_2$.

An analysis of the component E^f_{22} in the whole structure as function of time allows for concluding that E^f_{22} reaches its maximum values on sides 2 and 4. The component E^f_{22} of the fracture strain tensor measures the tendency of the structure to exhibit horizontal cracks in a certain region. Figures 10 and 11 show damage concentrated in the highest part of the structure, with a peak for $z = 36$ m. Although both referring to the E^f_{22} component, Figures 8 and 10 are not directly comparable, as the former regards a global parameter, while the latter refers to local strains. In any event, both figures show that the crack damage time-history is distributed mainly between 2 and 6 s. The three-dimensional model also enables detecting the emergence of vertical cracks, marked by the E^f_{11} component of the crack strain tensor. Figure 12 shows the component E^f_{11} at different heights of the tower, along side 3 of the tower: the maximum damage appears at a height of 27 m, about two thirds along the tower's height. It can also be noted (see Figures 11 and 12) that the order of magnitude of the E^f_{11} crack component is greater than that of the E^f_{22} component. As far as the crushing damage is concerned, as expected, it turns out to be concentrated at the tower's base. Figure 13 shows the component E^c_{22} of the crushing strain tensor vs. time, calculated at points B (at the base, in the middle of side 2) and C (at the base, corner between sides 2 and 3). Both the time-histories shown in Figures 9 and 13 highlight some damage peaks concentrated within very short time intervals. Finally, Figure 14 shows the values of T_{22}=$\mathbf{g}_2 \cdot \mathbf{T}\mathbf{g}_2$ at the base of the tower (point B) vs. time calculated by NOSA–ITACA and MADY codes.

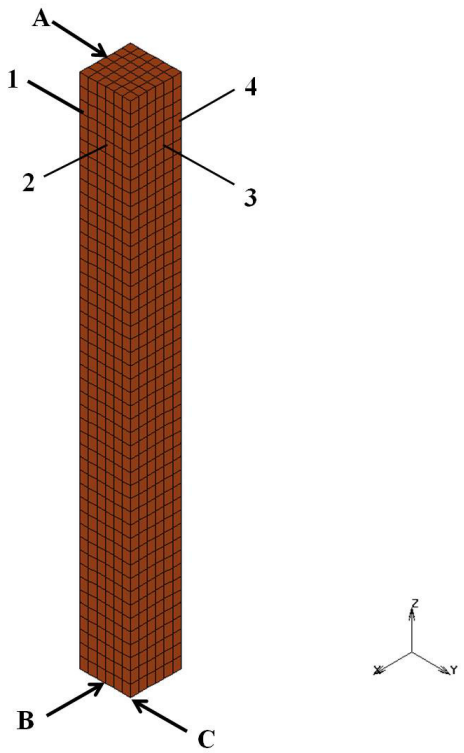

Figure 5: The masonry tower: finite element mesh.

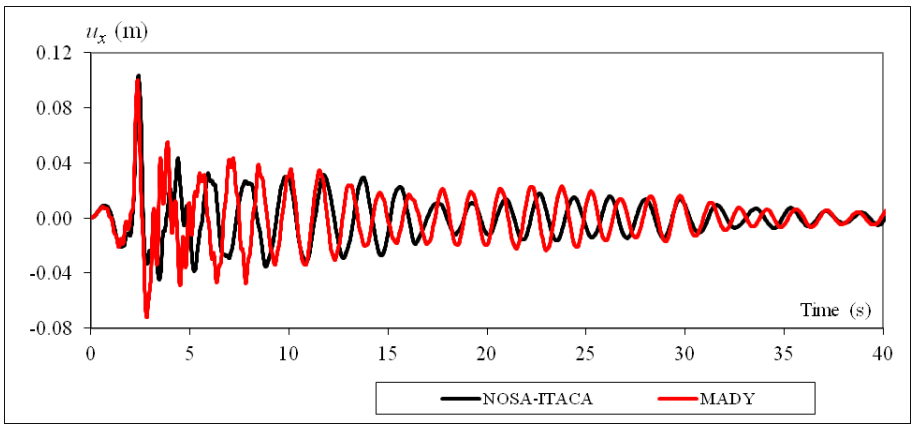

Figure 6: Relative $x-$ displacement u_x of point A vs. t.

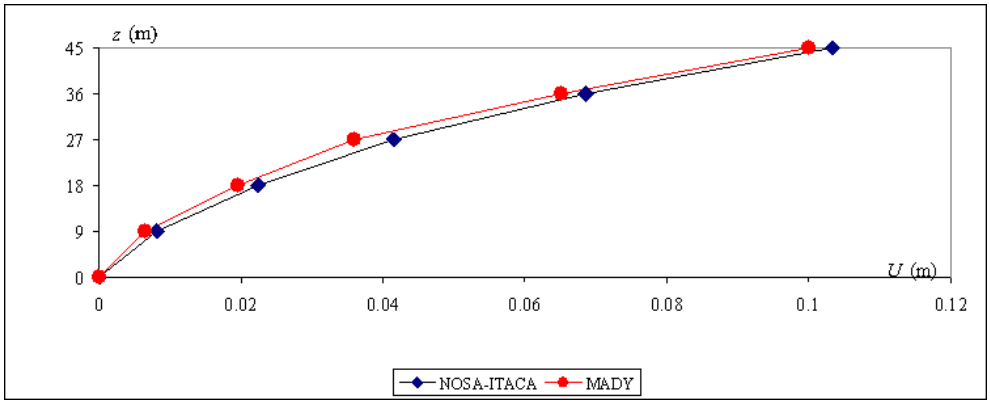

Figure 7: Maximum U of $\mid u_x \mid$ at $z = 9$ m, $z = 18$ m, $z = 27$ m, $z = 36$ m and $z = 45$ m.

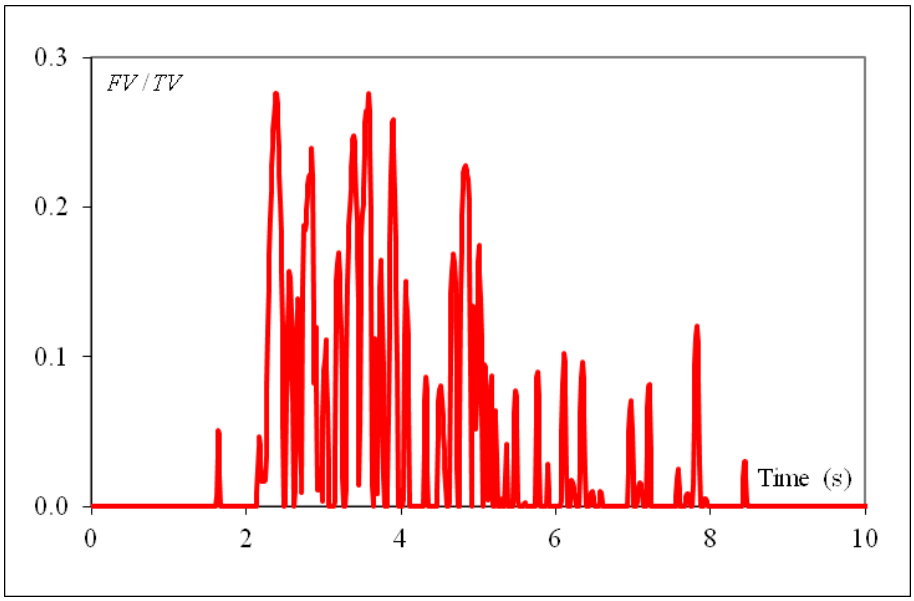

Figure 8: Plot of FV/TV vs. t (MADY).

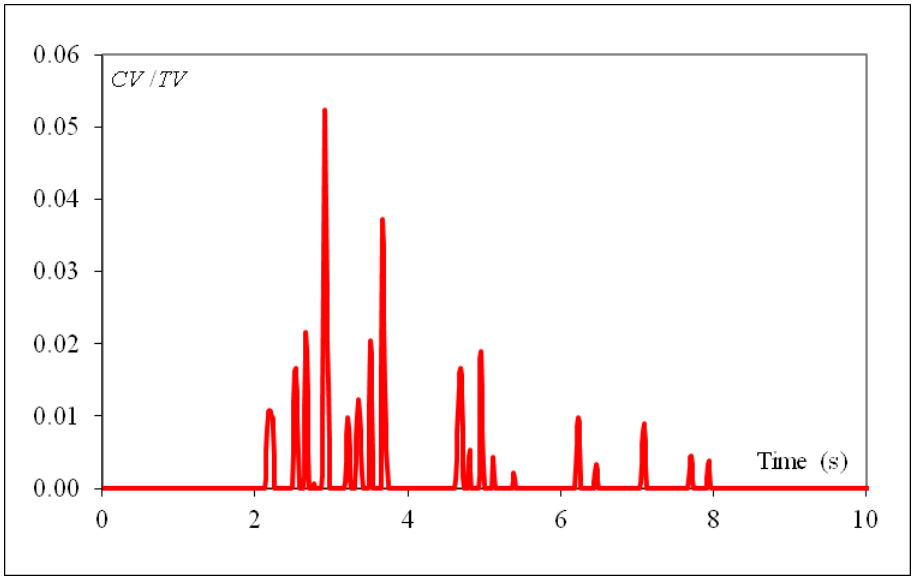

Figure 9: Plot of CV/TV vs. t (MADY).

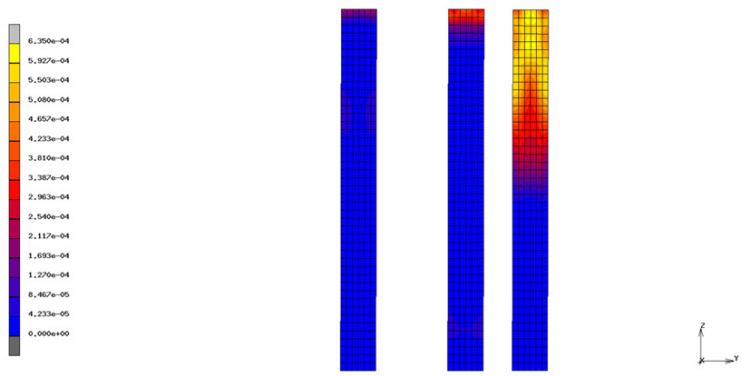

Figure 10: E_{22}^{f} values on side 2 at $t = 3.99$ s, $t = 4.24$ s and $t = 4.49$ s (NOSA–ITACA).

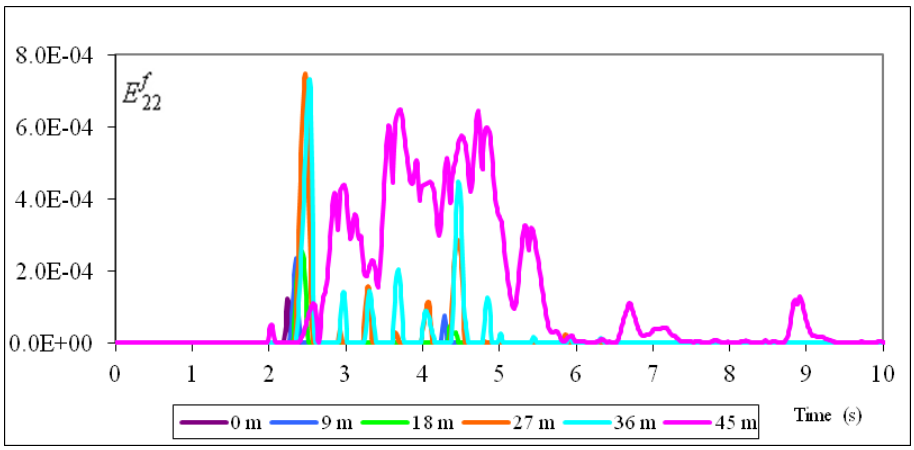

Figure 11: E^f_{22} vs. t at different levels of the tower (NOSA–ITACA).

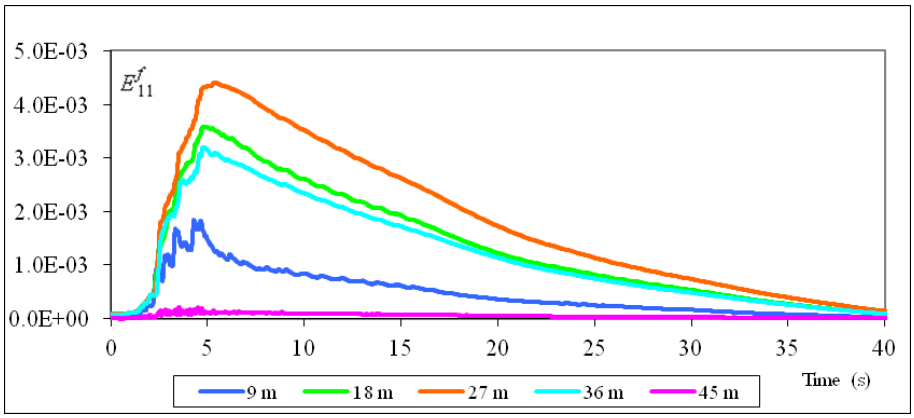

Figure 12: E^f_{11} vs. t at different levels of the tower (NOSA–ITACA).

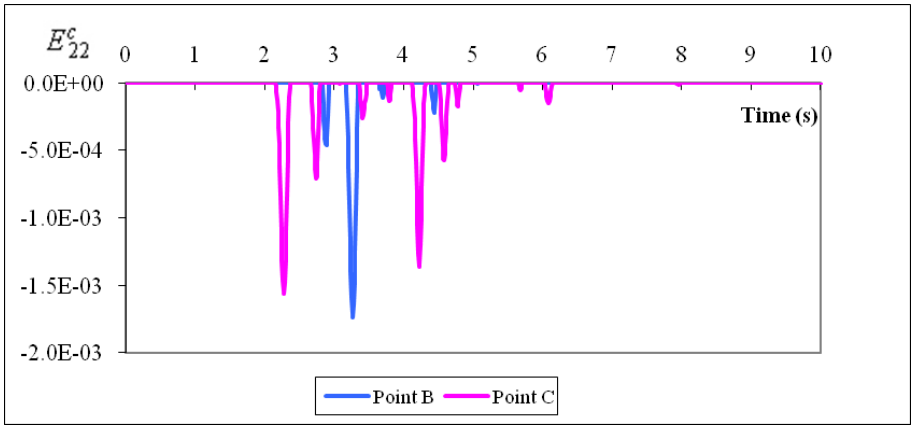

Figure 13: Values of E^c_{22} vs. t at the tower's base at points B (blue) and C (pink) (NOSA–ITACA).

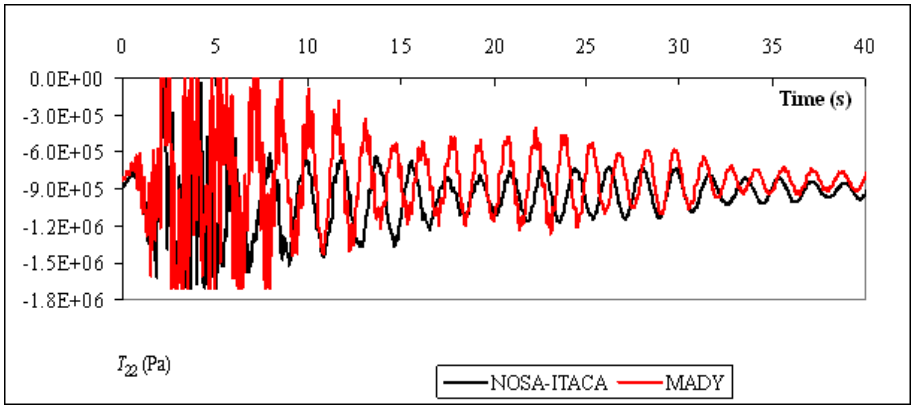

Figure 14: Values of T_{22} vs. t, calculated at the base of the tower.

4 Conclusions

This paper has presented two constitutive equations for three– and one–dimensional masonry structures. These constitutive equations view masonry as a nonlinear elastic materials with zero tensile strength and bounded compressive strength. These models, implemented in the finite-element codes NOSA–ITACA and MADY, enable investigating the dynamic behaviour of masonry structures. Here, in particular, they have been applied to the study of a masonry tower subjected to its own weight and a horizontal acceleration recorded during a real earthquake. By comparing the numerical solutions obtained via application of NOSA-ITACA and MADY, the consistencies and divergences between the two different approaches have been highlighted.

In particular, diplacements calculated by the two codes have turned out to be in good agreement. Different behaviours have been highlighted, instead, for the crack distribution: in fact, the MADY code takes into account only the flexural behaviour of the structure, while the results obtained using the NOSA–ITACA code, as a consequence of the three–dimensionality of the model, are also able to show the arise of vertical cracks.

Although these methods seem to capture many of the important dynamic properties of such structures quite well, they neglect other aspects, for example, those related to the irreversibility of the damage process, an aspect requiring further research and analysis.

Acknowledgements

This research was supported by the Region of Tuscany (project “Tools for modelling and assessing the structural behaviour of ancient constructions: the NOSA-ITACA code”, PAR FAS 2007-2013). This support is gratefully acknowledged.

References

[1] A.R. Selby, J.M. Wilson, ”The Dynamics of Masonry Bell Towers”, in J.W. Bull, (Editor), ”Computational Modelling of Masonry, Brickwork and Blockwork Structures”, Saxe-Coburg Publications, Stirlingshire, UK, Chapter 4, pp 79-108, 2001. doi:10.4203/csets.6.4

[2] Juhásová, E., Hurák,M. and Zembaty, Z., ”Assessment of seismic resistance of masonry structures including boundary conditions”, Soil Dynamics and Earthquake Engineering, 22, 1193–1197, 2002.

[3] Dogangun, A., Acar, R., Sezen, H., Livaoglu, R., ”Investigation of dynamic response of masonry minaret structures”, Bull Earthquake Eng, 6, 505–517, 2008.

[4] Papa, E. and Nappi, A., ”Numerical modelling of masonry: A material model accounting for damage effects and plastic strains”, Applied Mathematical Modelling, 21, 319–335, 1997.

[5] Giordano, A., Mele, E. , De Luca, A., ”Modelling of historical masonry structures: comparison of different approaches through a case study”, Engineering Structures, 24, 1057–1069, 2002.

[6] Mistler, M., Butenweg, C., Meskouris, K., ”Modelling methods of historic masonry buildings under seismic excitation”, J. Seismol., 10, 497–510, 2006.

[7] Pallarés, F. J., Agüero, Martín, A. M., ”Seismic behaviour of industrial masonry chimneys”, International Journal of Solids and Structures, 43, 2076–2090, 2006.

[8] Betti, M., Vignoli, A., ”Assessment of seismic resistance of a basilica-type church under earthquake loading: Modelling and analysis”, Advances in Engineering Software, 39, 258–283, 2008.

[9] P.B. Loureno, N. Mendes, R. Marques, ”Earthquake Design and Assessment of Masonry Structures: Review and Applications”, in B.H.V. Topping, L.F. Costa Neves, R.C. Barros, (Editors), ”Trends in Civil and Structural Engineering Computing”, Saxe-Coburg Publications, Stirlingshire, UK, Chapter 4, pp 77-101, 2009. doi:10.4203/csets.22.4

[10] Del Piero, G., ”Constitutive equation and compatibility of the external loads for linear elastic masonry-like materials”, Meccanica, 24, 150-162,1989.

[11] Di Pasquale, S., ”New trends in the analysis of masonry structures”, Meccanica, 27, 173-184, 1992.

[12] Lucchesi, M., Padovani, C., Pasquinelli, G., Zani, N., ”Masonry constructions: mechanical models and numerical applications”, Lecture Notes in Applied and Computational Mechanics 39, Springer-Verlag, Berlin Heidelberg, 2008.

[13] Degl’Innocenti, S., Padovani, C., Pasquinelli, G., ”Numerical methods for the dynamic analysis of masonry structures”, Structural Engineering and Mechanics, 22, 107-130, 2006.

[14] M. Callieri, M. Corsini, M. Girardi, C. Padovani, A. Pagni, G. Pasquinelli, R. Scopigno, ”The ”Rognosa” Tower in San Gimignano: Digital Acquisition and Structural Analysis”, in B.H.V. Topping, J.M. Adam, F.J. Pallars, R. Bru, M.L. Romero, (Editors), ”Proceedings of the Tenth International Conference on Computational Structures Technology”, Civil-Comp Press, Stirlingshire, UK, Paper

138, 2010. doi:10.4203/ccp.93.138
[15] Bathe, JK. J., Wilson, WE. L., ”Numerical methods in finite element analysis”, Prentice-Hall, Inc., Englewood Cliffs, New Jersey, 1976.
[16] Binante V., Girardi M., Padovani C., Pagni A., Pasquinelli G. ”The NOSA-ITACA code for the modelling of the structural behaviour of historic masonry constructions”. 5th International Congress on ”Science and Technology for the Safeguard of Cultural Heritage in the Mediterranean Basin” (Istanbul, Turkey, 22-25 november 2011).
[17] http://www.nosaitaca.it/
[18] http://www.salome-platform.org/
[19] Girardi M., Padovani C., Pasquinelli G. ”Numerical modelling of the dynamic behaviour of ancient masonry constructions”. WONDERmasonry 2011 - Workshop on Design for Rehabilitation of Masonry Structures (Florence, Italy, 10-11 November 2011).
[20] Zani, N., ”A constitutive equation and a closed-form solution for no-tension beams with limited compressive strength”, Eur. J. Mech. A/Solids, 23/3, 467-484, 2004.
[21] Lucchesi, M., Pintucchi, B., Zani, N., ”A model for vulnerability analysis of slender tower made of no tension material”, Proc. of the International Conference Earthquake Loss Estimation and Risk Reduction, Bucharest, Romania, 2002.
[22] Lucchesi, M., Pintucchi, B., ”A numerical model for non-linear dynamic analysis of slender masonry structures”, European Journal of Mechanics A/Solids, 26, 88-105, 2007.
[23] Lucchesi M., Padovani C., Silhavy M. ”An energetic view on the limit analysis of normal bodies”. Quarterly of Applied Mathematics, vol. 68 (4) pp. 713 - 746. American Mathematical Society, 2010.
[24] Gurtin, M. E., ”An introduction to continuum mechanics”, Academic Press, Boston, 1981.
[25] Silhavy M., Private Communication, 2007.
[26] Clough, R. W., Penzien, J., ”Dynamics of structures”, McGraw-Hill, 1975.